International Journal of Science and Research (IJSR)
ISSN: 2319-7064
Impact Factor (2018): 7.426

Hirshfeld Surface Analysis of Anisylresorcinarene and Luminescence Studies of its Benzimidazolyl Appended Ru(II) polypyridyl Complexes

Ligimol Louis, D. Suresh Kumar

Supramolecular Research Laboratory, Department of Chemistry, Loyola College, Chennai-600034, India

Abstract: ***The macrocyclic precursor, 2,8,14,20-tetrakis(4-methoxyphenyl)-4,6,10,12,16,18,-22,24-octahydroxycalix[4]resorcinarene (P1), has been synthesised and characterised using IR, NMR, ESI mass spectroscopy and single crystal X-ray diffraction analysis. P1 crystallizes in the monoclinic crystal system with $P2_1/c$ space group. Its Hirshfeld surface analysis has been carried out. The other precursor, 2-(pyridin-2-yl)-1H-benzimidazole (P2) and complex precursors, dichlorobis(phenanthroline)ruthenium(II) hydrate (P3) and dichlorobis(2,2'-bipyridine)ruthenium(II) hydrate (P4) are prepared by the modification of reported procedures. The macrocyclic ligand, benzimidazolyl functionalized anisylresorcinarene (L), has been synthesised by the aminomethylation of P1 using P2 and characterised using IR and ESI mass spectrometry. Tetranuclear ruthenium(II) phenanthroline and bipyridine complexes of L have been synthesized and characterized by IR, ESI-MS and electronic absorption spectroscopy. Upon excitation at the excitation maxima the complexes emit from the ^{3}MLCT state at 600 and 624 nm, respectively. The emission band of complexes at 77 K in frozen CH_3CN is hypsochromically shifted to 594 and 616 nm, respectively with noticeable increase in the emission intensity and in quantum yields. The complexes show monoexponential decay profile in acetonitrile and have life times of 142 and 200 ns, respectively.***

Keywords: Resorcinarene; Ru(II) complex;2-(pyridin-2-yl)-1*H*-benzimidazole; Hirshfeld surface analysis

1. Introduction

The coherent design and synthesis of novel architectures are of current interest in the field of supramolecular chemistry [1]. The resorc[n]arenes, which are calixarenes formed from resorcinol building blocks linked by methylene groups [2], are utilized as supramolecular assemblies which coordinate through all three of their constituent parts: the lower rim, the phenolic groups, and the *ortho* position on the aromatic rings [3]. Mannich reaction is one of the main reactions employed in functionalization of resorcinarenes with polypyridine ligands [4]. The rich photochemistry of polypyridine ligands, with almost all metals, is related with π-back bonding. The luminescent properties of ruthenium(II) complexes of phenanthroline and bipyridine have been extensively studied due to their significant MLCT absorption in the visible region, their ability to undergo MLCT excitations, and photoreactivity of the MLCT excited states [5]. The current investigation involves the synthesis, characterization and luminescence studies of tetranuclear ruthenium(II) bis(phenanthroline) and bis(bipyridine) complexes of benzimidazolyl functionalized anisylcalixresorcinarene. The Hirshfeld surface analysis of anisylresorcinarene crystal is also carried out to understand the intermolecular interaction present in the molecule.

2. Experimental Section

2.1 Reagents

Anisaldehyde, cyanopyridine, phenanthroline, 2,2′-bipyridine, ruthenium(III) chloride trihydrate, resorcinol, *o*-phenylenediamine, *o*-phosphoric acid, sodium perchlorate monohydrate (Aldrich), ammonia, hydrochloric acid (35%), and lithium chloride (Fluka) were purchased and used as such.

2.2 Physical measurements

Single-crystal X-ray structure data collections were performed on a Bruker AXS Kappa Apex II CCD diffractometer with graphite monochromatic Mo (Kα) radiation (λ) 0.71073 Å). Infrared spectra were recorded on a Perkin-Elmer spectrum RX-I FT-IR Spectrometer in the range of 4000-400 cm^{-1}. The electrospray ionization mass spectra were recorded on a micromass Quattro II triple quadrupole mass spectrometer. ^{1}H NMR was recorded on a Bruker AVANCE III 500 MHz (AV 500) multinuclear NMR spectrometer at 25 ºC. The electronic absorption spectra were recorded on a Shimadzu UV-2450 UV-Visible spectrophotometer controlled by the UV Probe version-2.33 software. Fluorescence spectra were recorded on a Fluorolog-3 FL3-221 spectrofluorometer. The emission lifetimes were carried out using nanosecond laser flash photolysis (Applied Photophysics, U.K.). Emission quantum yields (Φ) were calculated by integrating the area under the luminescence curves and by using equation 1 [6] where OD is optical density of the compound at the excitation wavelength and A is the area under the emission spectral curve. The standard used for the luminescence quantum yield measurements was $[Ru(bpy)_3]Cl_2$ (Φ =0.04) [7] and corrected for the refractive index of the solvent.

$$\Phi = \{OD_{std}A_{sample}\eta^2_{sample}\}/\{OD_{sample}A_{std}\eta^2_{std}\}\Phi_{std} \quad \text{Eq.1}$$

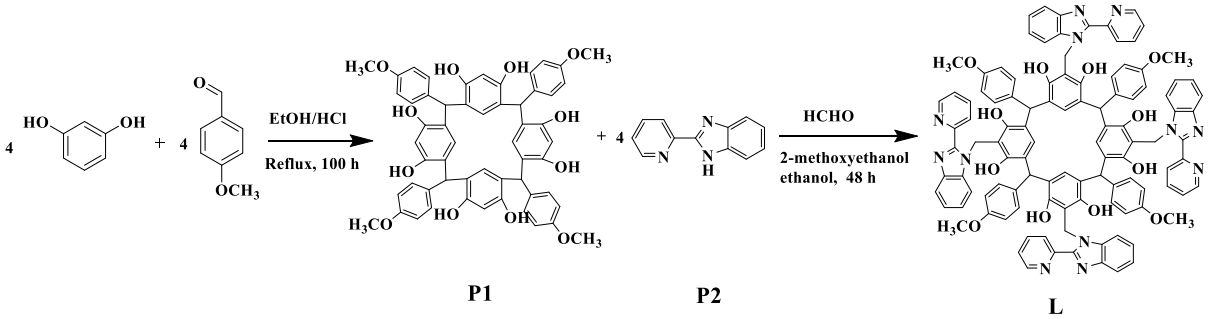

Scheme 1: Synthesis of anisylresorcinarene (P1) and the ligand (L)

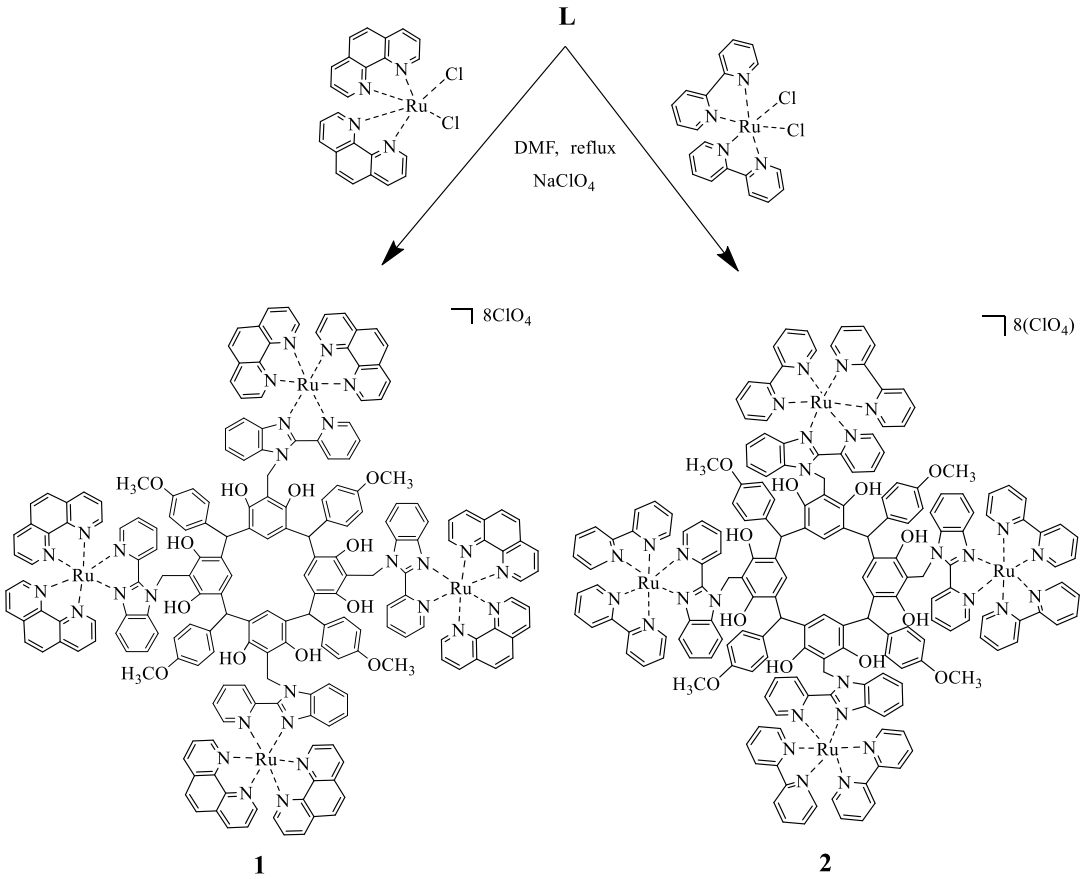

Scheme 2: Synthesis of tetranuclear ruthenium(II) complexes of L

2.3 Synthesis of precursor, anisylcalix[4]resorcinarene (P1)

To a solution of resorcinol (2.75 g, 25 mmol) in ethanol-water (7:3 v/v, 50 mL), was added hydrochloric acid (35%, 10 mL) stirred at 70 °C for 1 h. A solution of anisaldehyde (3.04 g, 25 mmol) in ethanol (50 mL) was added to the reaction mixture followed by water (30 mL). The resulting suspension was refluxed under stirring for 100 h and then cooled to room temperature. The solid product that separated out was filtered, washed with water, and dried to obtain a pale orange powder. The product formed was recrystallized in DMF and characterised.

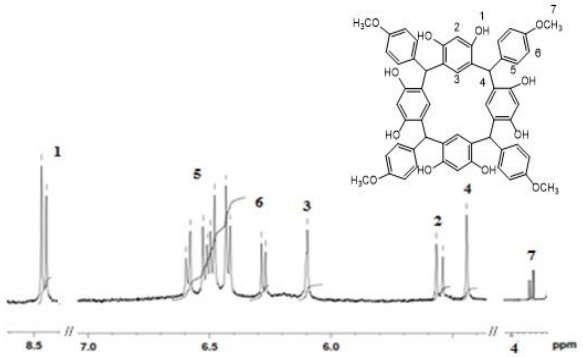

Figure 1: 500 MHz ^{1}H NMR spectrum of **P1** in DMSO-d_6 at 25°C

Yield 4.85 g (85%), pale yellow powder, mp> 300 °C (dec.). Analytical data calculated for $C_{56}H_{48}O_{12}$ (M_r = 913): C, 73.21; H, 5.18. Found: C, 73.67; H, 5.30. IR data ν_{max}/cm^{-1} 3373 ν(O–H), 2932 ν(C–H) (aromatic), 2833 ν(C–H)

(aliphatic), 1658, 1608 and 1510 ν(C=C) (aromatic), 1430 δ(C–H) (aliphatic), 1247 ν(C–O), 822 γ(C-H) (aromatic). ^{1}H NMR data (500 MHz, DMSO-d_6, 298 K) δ 5.44 (4H, s, *CH*), 5.55 (4H, d), 6.09 (4H, s,), 6.27 (8H, d,), 6.50 (8H, m), 8.45 (8H, m). ESI MS: *m/z* 913 $[M]^+$, 936 $[M+Na]^+$.

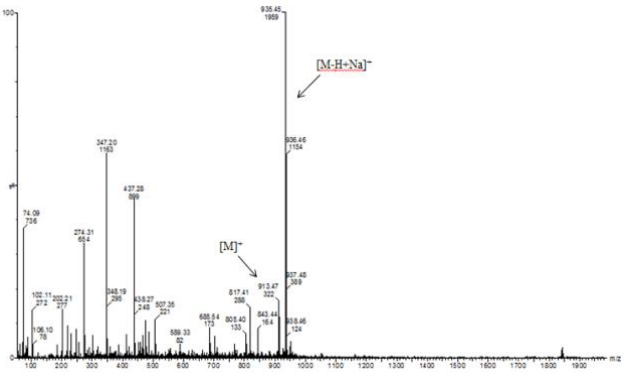

Figure 2: ESI-TOF mass spectrum of **P1**

2.4 Synthesis of ligand (L)

To a solution of **P1** (1 g, 1.09 mmol) and 2-(pyridin-2-yl)-1*H*-benzimidazole (**P2**) (0.85 g, 4.38 mmol) in a solvent mixture of 2-methoxyethanol-ethanol (2:1 v/v, 60 mL), was added 37% aqueous solution of formaldehyde (0.12 ml, 4.38 mmol) under argon atmosphere and refluxed for 48 h. The resulting solution was flash evaporated to get red precipitate and recrystallized.

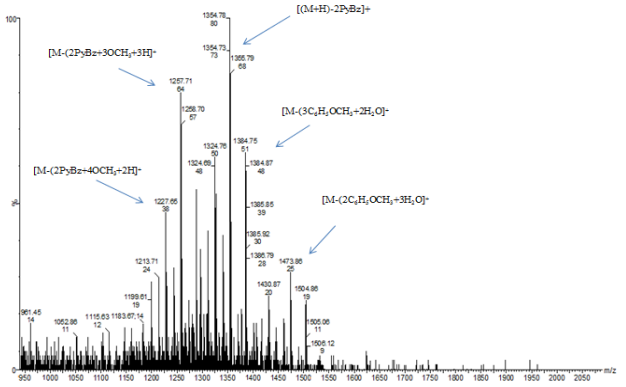

Figure 3: ESI-TOF mass spectrum of **L**.

Yield 6.3 g (72 %) Red powder, Mp>300 °C (dec.). Analytical data calculated for $C_{108}H_{84}N_{12}O_{12}$ (M_r = 1741): C, 74.47; H, 4.86; N, 9.65. Found: C, 74.35; H, 4.68; N, 9.58. IR spectrum: ν(cm^{-1}) 3316 ν(O-H), 2926 ν(C-H) (aromatic), 2833 ν(C-H) (aliphatic), 1605, 1510 ν(C=C) (aromatic), 1466 δ (CH_2-N), 1246 ν(C–O), 745 ω(-CH_2). ESI MS: ESI MS: *m/z* 1227 $[M-(2\mathbf{P2}+4OCH_3+H]^+$; 1257 $[M-(2\mathbf{P2}+3OCH_3+H]^+$; 1354 $[(M+H)-2\mathbf{P2}]^+$.

2.5 Synthesis of tetranuclear ruthenium(II) polypyridyl complexes, $[\{Ru(phen)_2Cl\}_4(L)](ClO_4)_8$ (1), and $[\{Ru(bpy)_2Cl\}_4(L)](ClO_4)_8$ (2)

A solution of the ligand L (0.17 g, 0.10 mmol) and $[Ru(phen)_2Cl_2]\cdot 2H_2O$ (0.21 g, 0.4 mmol) or $[Ru(bpy)_2Cl_2]\cdot 2H_2O$ (0.20 g, 0.4 mmol) in DMF (50 mL) was refluxed with stirring under an argon atmosphere for 12 h. The resultant dark suspension was cooled and filtered. The volume of the filtrate was reduced to 5 mL and 50 mL of sodium perchlorate solution was added with stirring whereupon a dark red solid separated out. The product was filtered, dried and recrystallized in hot acetonitrile.

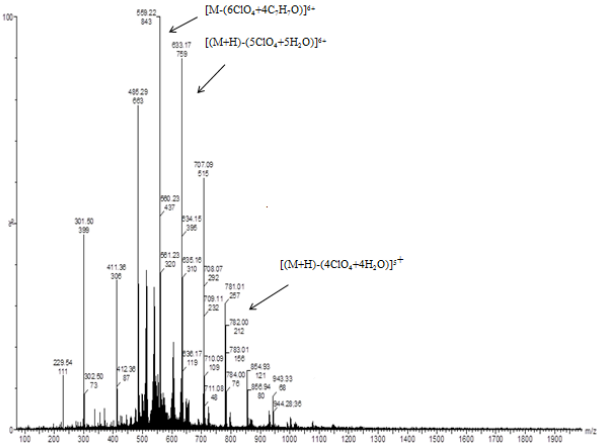

Figure 4: ESI-MS spectrum of complex **1**.

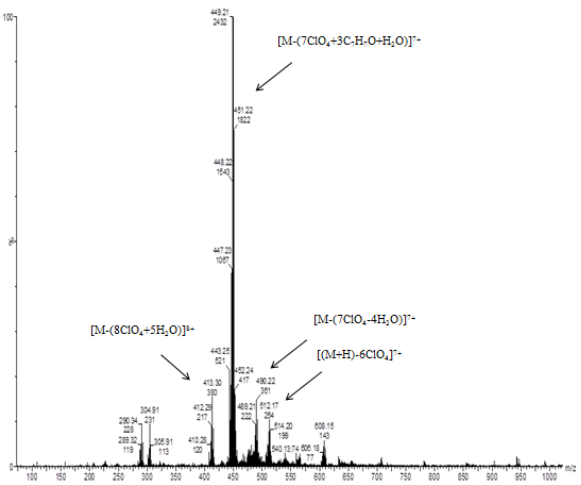

Figure 5: ESI mass spectrum of **2.**

1 - Yield 0.32 g, (74%), Dark red solid. Analytical data calculated for $C_{204}H_{148}N_{28}O_{44}Cl_8Ru_4$ (M_r = 4383.42): C, 55.90; H, 3.40; N, 8.95. Found: C, 55.75; H, 3.34; N, 8.91. IR data: ν_{max}/cm^{-1} 3430 ν(O–H), 3066 ν(C–H) (aromatic), 2924 ν(C-H) (aliphatic), 1609 and 1516 ν(C=C) (aromatic), 1426 δ(C-H) (aliphatic), 1097 ν(ClO_4), 846 γ(C-H) (aromatic) 753 ω(C-H). ESI MS: *m/z* 559 $[(M-(6ClO_4+4C_7H_7O)]^{6+}$, 633 $[(M+H)-5ClO_4+5H_2O)^{6+}$, 781 $[(M+H)-(4ClO_4+4H_2O]^{4+}$.

2 - Yield 0.31 g (75%), Dark red solid. Analytical data calculated for $C_{188}H_{148}N_{28}O_{44}Cl_8Ru_4$ (M_r = 4191.25): C, 53.88; H, 3.56; N, 9.36. Found: C, 66.38; H, 4.13; N, 11.43. IR data: ν_{max}/cm^{-1} 3417 ν(O–H), 3069 ν(C–H) (aromatic), 2920 ν(C-H) (aliphatic), 1602 and 1509 ν(C=C) (aromatic), 1444 δ(C-H) (aliphatic), 1088 ν(ClO_4), 763 ω(C-H). ESI MS: *m/z* 413 $[(M-(8ClO_4+5H_2O)]^{8+}$, 449 $[M-(7ClO_4+3C_7H_7O+H_2O)]^{7+}$ 490 $[M-7ClO_4+4H_2O)^{7+}$, 512 $[(M+H)-6ClO_4]^{7+}$.

3.1 Synthesis and Characterisation of organic precursors, ligand and complexes.

The acid catalyzed condensation of resorcinol (1 equiv) with 4-methoxybenzaldehyde (1 equiv) upon refluxing in ethanol-water mixture gives **P1** (Scheme 1). It is characterized by CHN analysis, IR, NMR, ESI mass spectroscopy and single crystal x-ray diffraction analysis. The absence of aldehyde (C=O) stretching vibration and presence of intermolecular hydrogen bonded hydroxyl (-OH) stretching in FT-IR spectrum of **P1** confirms the condensation reaction. The ^{1}H NMR spectrum shows resonance signals for aromatic, hydroxyl, methoxy and methine bridge protons (Figure 1). The mass spectrum of **P1** shows a peak at *m/z* 913 due to molecular ion species, $[M]^+$ ($C_{56}H_{48}O_{12}$) (Figure 2). The compound 2-(pyridin-2-yl)-1*H*-benzimidazole (**P2**) was prepared by the condensation of equimolar amount of 2-cyanopyridine and *o*-phenylenediamine in *o*-phosphoric acid by using the modified procedure reported by Addison [8]. The benzimidazolyl pyridine functionalized anisylcalix[4]resorcinarene (**L**) was synthesized by the reaction of anisylcalix[4]resorcinarene (**P1**) with 2-(pyridin-2-yl)-1*H*-benzimidazole (**P2**) and formaldehyde in solvent mixture of ethanol and 2-methoxyethanol (Scheme 1). The ligand **L** is characterized by CHN analysis, IR, and mass spectrometry. In FT-IR spectrum of **L**, the band at 1466 cm^{-1} is due to scissoring of -CH_2- connected to tertiary amine, confirming the formation of CH_2 bridge in the ligands. The ESI-TOF mass spectrum of **L** shows a peak at *m/z* 1473 corresponding to the fragment $[M-(2C_6H_5OCH_3+3H_2O]^+$ formed by the removal of two methoxyphenyl groups and three water molecules from the molecular ion. The peak at m/z 1354 is due to the fragment $[(M+H)-2\mathbf{P2}]^+$ formed by the loss of two benzimidazolyl pyridine groups followed by the addition of one hydrogen atom to the molecular ion (Figure 3). The precursor complexes, $[Ru(phen)_2Cl_2].2H_2O$ (**P3**) and $[Ru(bpy)_2Cl_2].2H_2O$ (**P4**) were synthesized by the reaction of $RuCl_3.3H_2O$ (1 equiv) and phenanthroline or bipyridine (2 equiv) in refluxing DMF in the presence of lithium chloride as reported by Sullivan et al [9].

The reaction of ruthenium precursor complexes, **P3** or **P4,** with the ligand **L** (1 equiv) in N,N-dimethylformamide, as per the Scheme 2, formed the stable complexes of **1** and **2**, respectively. The tetranuclear complexes were characterized by CHN analysis, IR, ESI MS, and electronic absorption spectroscopy. The IR spectral bands at 1097 and 1088 cm^{-1} confirm the presence of perchlorate counter ion in complexes **1** and **2**, respectively. The ESI-TOF mass spectra of the complexes give the peaks corresponding to the fragmented ions of the complexes (Figure 4 and 5).

3.2 Crystal structure of P1

The ORTEP representation of **P1** with all atoms presented as 40% probability ellipsoid is given in Figure 6. The compound **P1** crystallizes in monoclinic crystal system with $P_{21/C}$ space group. The cell parameters are a = 17.4950(5) Å, b = 11.6056(3) Å, c = 19.7364(6) Å, α = γ = 90°, β = 74.923(3)°, V = 3630.4(3) $Å^3$ and Z = 2. The molecule possesses a cis-trans-trans (ctt) configuration and a rigid chair-like conformation. The asymmetric unit is comprised of half of the anisylresorcinarene molecule which can be completed using the two fold rotation axis (axis passing through the centre of the molecule). The solvent molecules are found to be highly disordered throughout the crystal lattice and so they are removed using SQUEESE program. The resorcinol hydroxyl groups are found to involve in the intermolecular H-bonding with the -OCH_3 group of the nearby molecule that the C-H···O interactions between the two molecules also stabilise the crystal lattice (Figure 7).

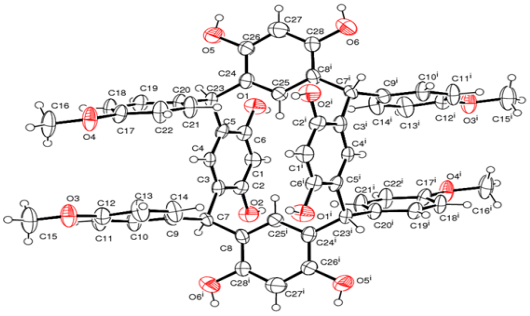

Figure 6: ORTEP representation of **P1** (CCDC # 1566460) with atoms represented as 40% probability thermal ellipsoids.

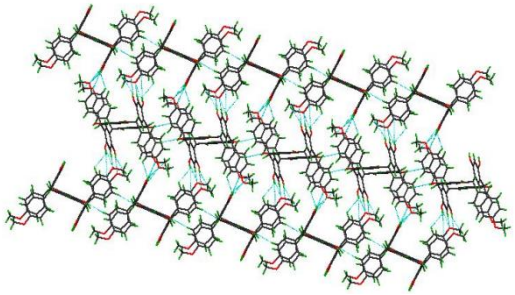

Figure 7: Two dimensional arrangement of **P1** crystal with short contacts

3.3 Hirshfeld surface analysis of P1

Intermolecular interactions play a vital role in the crystal packing of molecules in supramolecular chemistry. The quantitative measurements of these interactions are possible by Hirshfeld surface (HS) analysis of the crystal [10]. The HSs of **P1** in the Figure 8 show surfaces that have been mapped with d_{norm}, shape index and curvedness. The intense red spots in the d_e surface near to resorcinol ring are due to H-bond interaction present in the molecule and the light red spots are due to C-H and CH-π interactions.

The shape index map on the HSs shows a complementary red hollows and blue bumps where two molecular HSs touch one another. Curvedness shows relatively large regions of green with root mean square (r.m.s.) curvature near unity, which is separated by dark blue `edges' with large r.m.s. curvature. Occasional highlights of yellow and red indicate hydrogen bonds on the surface. The quantitative measures like volume (V_H), area (S_H), globularity (G) and asphericity (Ω) were also computed using HS analysis. The term, globularity (G) is found to be <1 which indicates that the molecular surface is more structured, not a sphere. The asphericity, the measure of anisotropy [10] is found to be 0.11 for P1.

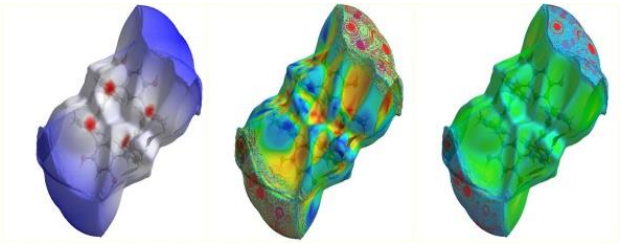

Figure 8: Hirshfeld surfaces of P1(d_{norm}, shape index and curvedness).

3.4 Fingerprint plots of P1

Two dimensional summaries of the intermolecular interactions in the crystal system are provided by a finger print plot of d_e versus d_i. Figure 9 displays the two dimensional finger print plots for the P1 molecule which involve features like spike of various length and thickness corresponding to all the intermolecular interaction present within the crystal structure. The wing like peripheral spikes represent C-H contacts in finger print plot whereas hydrogen bonding are present as longer and thinner spikes and the non-directional H···H contacts are characterized by broader spikes.

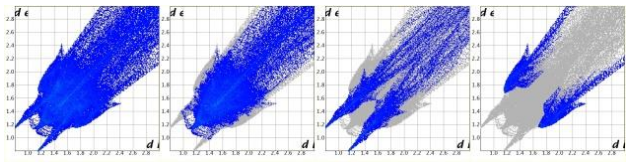

Figure 9: Fingerprint regions of **P1** (all interactions-100%, H-H -72.9%, O-H-19.9%, C-H 7.3%).

3.5 Luminescence properties of complexes at 298 and 77 K.

The tetranuclear ruthenium(II) complexes exhibit electronic absorption bands at 263, 317 and 332 nm for **1**, and 289, 317 and 333 nm for **2** assignable to the ligand centered π-π* transitions and broad absorption bands at 445 and 457 nm for **1** and **2**, respectively, characteristic of the ^{1}MLCT transition.

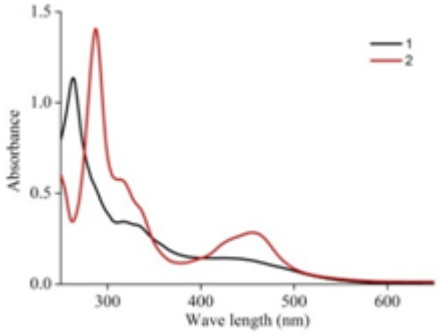

Figure10: Electronic absorption spectra of the complexes **1** and **2** in CH_3CN at 298K.

The emission spectra of the complexes were recorded in CH_3CN at 298 K and 77 K. Upon excitation onto their excitation maxima, **1** and **2** complexes exhibit emission bands at 600 and 624 nm, respectively due to ^{3}MLCT emission at 298 K. The complexes show blue shift in emission maxima in comparison with the parent compound $[(bpy)_2Ru(\mathbf{P4})]^{2+}$ [11]. The emission band of complexes **1** and **2** at 77 K in frozen CH_3CN is hypsochromically shifted to 594 and 616 nm, respectively with noticeable increase in the emission intensity due to rigidochromic effect which is characteristic of typical MLCT emitters [12]. The quantum yields of **1** and **2** have increased from 0.003 to 0.04; and 0.013 to 0.23, respectively, when the temperature is decreased from 298 K to 77 K. The complexes show monoexponential decay profile in acetonitrile and have life time of 142 and 200 ns for **1** and **2**, respectively. The absorption and emission spectra are depicted in Figures 10 and 11, respectively.

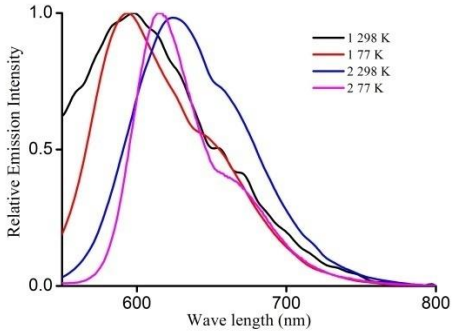

Figure 11: Emission spectra (normalised) of complexes **1** and **2** in CH_3CN at 298K and 77K.

4. Conclusion

A new benzimidazolyl functionalized anisylcalix[4]-resorcinarene and its tetranuclear Ru(II) polypyridyl complexes have been prepared. The study demonstrates the versatility of calixresorcinarenes in the assembly of polynuclear ruthenium(II) complexes. The methodology developed in the present work can be exploited to synthesize a series of polypyridine functionalized calixresorcinarenes. The tetranuclear Ru(II) complex is stable in solution and solid state under ambient conditions and is reasonably soluble in organic solvents. The ligand offers a wide scope in constructing a plethora of complexes by inserting different metal cations to vary and fine-tune the electronic properties in such polynuclear assemblies.

Acknowledgements

The authors gratefully acknowledge the services of SAIF, IIT-Madras, Chennai for NMR spectra and XRD; SAIF, Punjab University, Chandigarh for ESI-MS; and NCUFP, University of Madras, Chennai for the emission lifetime measurements.

References

[1] Lehn, J.-M., "Toward complex matter: Supramolecular chemistry and self-organization", *Proc. Nat. Acad. Sci.*, USA, **2002**, *99*, 4763-4768.
[2] Böhmer, V., "Calixarenes, macrocycles with (almost) unlimited possibilities", *Angew. Chem. Int. Ed. Engl.*, **1995**, *34*, 713-745.

[3] Fairfull-Smith, K.; Redon, P. M. J.; Haycock, J. W.; Williams, N. H., "Monofunctionalised resorcinarenes", *Tetrahedron Lett.*, **2007**, *48*, 1317-1319.
[4] Arend, M.; Westermann, B.; Risch, N., "Modern variants of the Mannich reaction", *Angew. Chem. Int. Edn.*, **1998**, *37*, 1044-1070.
[5] (a) Anderson, P. A.; Keene, F. R.; Meyer, T. J.; Moss, J. A.; Strouse, G. F.; Treadway, J. A., "Manipulating the properties of MLCT excited states", *J. Chem. Soc., Dalton Trans.*, **2002**, 3820−3831. (b) Vogler, A.; Kunkely, H., "Photoreactivity of metal-to-ligand charge transfer excited states", *Coord. Chem. Rev.*, **1998**, *177*, 81−96.
[6] Ishida, H,; Tobita, S.; Hasegawa, Y.; Katoh, R.; Nozaki, K., "Recent advances in instrumentation for absolute emission quantum yield measurements", *Coord. Chem. Rev.*, **2010**, *254*, 2449–2458.
[7] Lakowicz, J. R. *Principles of Luminescence Spectroscopy, 3rd ed*.; Springer, New York, 2006.
[8] Addison, A.W.; Burke, P.J, "Synthesis of some imidazole-and pyrazole-derived chelating agents", *J. Het. Chem*., **1981**, *18*, 803−804.
[9] Sullivan, B. P.; Salmon, D. J.; Meyer, T. J., "Mixed phosphine 2,2'-bipyridine complexes of ruthenium", *Inorg. Chem.*, **1978**, *17*, 3334-3341.
[10] Gilewska, A.; Masternak, J.; Kazimierczuk, K.; Trynda, J.; Wietrzyk, J.; Barszcz, B., "Synthesis, structure, DNA binding and anticancer activity of mixed ligand ruthenium (II) complex", *J. Mol. Struct*., **2018**, *1155*, 288-296.
[11] Hunan, Y.; Joe, A. C.; John, T. S. I., "Ruthenium complexes of 2-(2′-pyridyl)benzimidazole as photosensitizers for dye-sensitized solar cells", *Dalton. Trans.* **2003**, *4*, 685-691.
[12] Watts, R. J.; Missimer, D., "Environmentally hindered radiationless transitions between states of different orbital parentage in iridium(III) complexes. Application of rigid-matrix induced perturbations of the pseudo-Jahn-Teller potential to the rigidochromic effect in d_6 metal complexes", *J. Am. Chem. Soc*., **1978**, *100*, 5350-5357.